Crystal Structures and Photophysical Properties of 9-Anthracene Carboxylic Acid Derivatives for Photomechanical Applications

ARTICLE *in* CRYSTAL GROWTH & DESIGN · SEPTEMBER 2011

Impact Factor: 4.89 · DOI: 10.1021/cg200883b

CRYSTAL GROWTH & DESIGN

ARTICLE

pubs.acs.org/crystal

Crystal Structures and Photophysical Properties of 9-Anthracene Carboxylic Acid Derivatives for Photomechanical Applications

Lingyan Zhu,[†] Rabih O. Al-Kaysi,[‡] Robert J. Dillon,[†] Fook S. Tham,[†] and Christopher J. Bardeen*[,†]

[†]Department of Chemistry, University of California, Riverside, Riverside, California 92521, United States

[‡]College of Basic Sciences, King Saud bin Abdulaziz University for Health Sciences-National Guard Health Affairs, Riyadh 11426, Kingdom of Saudi Arabia

Supporting Information

ABSTRACT: Molecular crystals composed of 9-anthracene carboxylic acid (9AC) can undergo reversible light-induced mechanical motions driven by a [4 + 4] photodimerization reaction. This paper explores the structure, photophysics, and photomechanical response of a family of anthracene carboxylic acid derivatives, with the goal of finding materials that have comparable or improved photomechanical properties. We find that methyl or phenyl substitution at the 10-position leads to a complete loss of photoreactivity due to changes in crystal packing. A series of halogen (F, Cl, Br) 10-substituted 9AC molecules all showed a similar stacked packing motif, but only the fluoro-substituted molecule was photoreactive in the solid. Its photomechanical response was similar to that of 9AC but with a much longer recovery time. Extending the carboxylic acid by adding a vinylene group at the 9-position resulted in crystals that showed good photoreactivity and a lack of fracture but no reversibility. Attempts to self-consistently rationalize observed trends in terms of excited state lifetimes or steric effects were only partly successful. Balancing factors such as electronic relaxation, steric interactions, and crystal packing present a challenge for engineering photoactive solid-state materials based on molecular crystals.

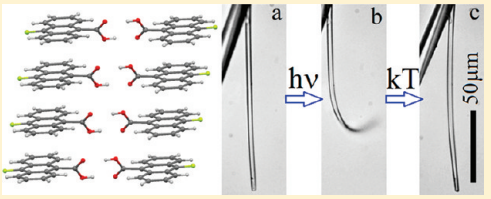

INTRODUCTION

Photomechanically responsive organic materials provide a way to transform photon energy directly into mechanical energy. While much work has focused on polymers and liquid crystal elastomers,[1−3] molecular crystals are also beginning to attract attention as possible photomechanical materials.[4−9] Previous work in our research group has focused on using the [4 + 4] photodimerization of anthracene derivatives to induce deformations in molecular crystal nanorods.[10,11] For a material to have potential as an actuator, the photochemical reaction should be reversible, either by ambient thermal fluctuations or by exposure to a different wavelength of light. The molecule 9-anthracene carboxylic acid (9AC), which crystallizes in an unusual head-to-head conformation driven by hydrogen bonding, forms a metastable photodimer that spontaneously dissociates back into its constituent monomers.[12] Using this molecule, we have demonstrated controlled bending of crystalline nanorods[13−15] and the twisting of microribbons,[16] where both types of motion spontaneously reverse over the course of minutes. Although this type of reversibility is robust and can be used for multiple cycles of light-induced shape changes, we became interested in whether we could develop systems with improved photomechanical responses. In particular, we wanted to decrease the recovery time of the actuator by accelerating the dissociation of the photodimer. We hypothesized that one way to accomplish this would be to modify the chemical substituents at the 9 or 10 position of the anthracene ring, thereby increasing the steric repulsion between the two halves of the photodimer.

In this paper, we report the synthesis and characterization of a series of 9AC derivatives in both solution and in the solid state. The seven compounds that are the subject of this paper are shown in Scheme 1. Compounds **1**−**6** represent an attempt to explore how substitution at the 10-position opposite the COOH group influences both crystal packing and chemical reactivity. Compound **7** is an attempt to modify the COOH attachment at the 9-position. In all cases, we find that the hydrogen bonding of the COOH groups plays an important role in determining the crystal packing, but that the crystal structures still vary quite a bit once the 10-position substituent becomes more complicated than a single atom. For the single atom series **1**−**4**, we find that only H and F substituents at the 10-position result in photochemically reactive solids, while larger atoms or molecular substituents appear to prevent the dimerization reaction altogether. If we leave the 10-position alone and modify the 9-position (compound **7**), photoreactivity is retained but reversibility is lost. Thus, although it is possible to tune the solid-state reactivity of 9AC somewhat through chemical substitution, unsubstituted 9AC still appears to be the best photomechanical material in terms of reactivity, ease of growth, and reversibility.

Received: July 12, 2011
Revised: August 30, 2011

dx.doi.org/10.1021/cg200883b | *Cryst. Growth Des.* XXXX, XXX, 000–000

Scheme 1. 9-Anthracene Carboxylic Acid Derivatives Studied in This Work

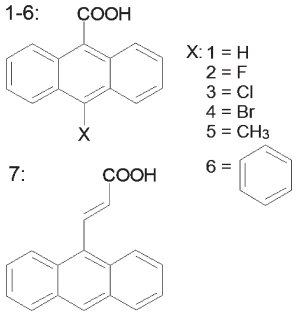

EXPERIMENTAL SECTION

1. Materials. 9-Anthracene carboxylic acid (9AC, **1**) was purchased from Sigma Aldrich (99%) and used after recrystallization from CH_2Cl_2. 1-Anthracenecarboxylic acid (>99%) and 2-anthracenecarboxylic acid (>98%) were purchased from TCI and used after recrystallization from ethanol. Compounds **2**−**7** were synthesized using modified literature procedures. The detailed synthetic procedure and characterization of all compounds are provided in the Supporting Information.

2. Crystal Growth. *Compounds **1** and **5**.* These crystals were grown by slow solvent evaporation. For monoclinic **1**, 5.7 mg of **1** was dissolved in 1.0 mL of filtered ethyl acetate in an 8 mL glass vial, with gentle heating. The vial was sealed with a polyethylene lid, and the lid was pierced by a needle. After the ethyl acetate evaporated through the needle over the course of several days, single crystals of monoclinic **1** were collected from the bottom of the glass vial. For triclinic **1**, 5.5 mg of **1** was dissolved in 2.0 mL of filtered xylenes in an 8 mL glass vial. The vial was again sealed with a polyethylene lid pierced by a needle. After the xylenes evaporated over the course of several days, single crystals of triclinic **1** were collected from the bottom of the glass vial. To grow crystals of **5**, 1.0 mg of **5** was dissolved in 0.1 mL of DMSO in a well-plate and covered by aluminum foil. Single crystals of **5** were collected after several days.

*Compounds **2**−**4**, **6**, **7**.* For these compounds, we used a modified sublimation procedure. 2.5 mg of a powdered derivative was placed at the center of the bottom of a glass vial. Three glass cylinders, 1 cm in diameter by 1 cm tall, were then stacked on top of each other, with the powder in the center. The glass vial was sealed in air with a glass lid, covered with a beaker wrapped with aluminum foil, and heated to 200 °C. After sublimation for about 15 h, the bottom cylinder contained needle-shaped crystals, and single crystals were collected from the upper part of the bottom cylinder. The middle cylinder typically had few if any crystals, while the top cylinder contained volatile impurities that were discarded.

3. X-ray Diffraction Measurements. Single-crystal X-ray diffraction data were collected on a Bruker APEX2 platform CCD X-ray diffractometer system (Mo-radiation, λ = 0.71073 Å, 50 kV/40 mA power) at 296 and 100 K. The frames were integrated using the Bruker SAINT software package and a narrow-frame integration algorithm. Absorption corrections were applied to the raw intensity data using the SADABS program. The Bruker SHELXTL software package was used for phase determination and structure refinement.[17−20] Powder X-ray diffraction data were collected on a Bruker D8 Advance X-ray powder diffractometer (CuK radiation, λ = 1.5418 Å, 40 kV/40 mA power) at 296 K.

4. Time-Resolved Fluorescence Measurements. Time-resolved fluorescence lifetime data on single crystals were collected with a Hamamastsu C4334 Streakscope. The solid samples were kept under a vacuum in a Janis ST100 cryostat. Two sets of data were collected using different excitation sources: a 1 kHz Coherent Libra and a 40 kHz Spectra Physics Spitfire laser system. In both cases, the 800 nm output pulse was frequency doubled to 400 nm and residual 800 nm light was removed with dichroic mirrors and Schott glass BG39 filters. The per-pulse excitation fluences used were less than 50 nJ/cm^2. All fluorescence was detected at a polarization angle set to 54.7° (the magic angle) relative to the excitation polarization.

5. UV−vis Absorption and Steady-State Fluorescence Measurements. UV−vis absorption spectra were collected on a Varian Cary 50 UV/vis spectrophotometer from 200 to 500 nm at 296 K with background subtraction. Tetrahydrofuran (THF) was used as the solvent for the solution samples. The thin films for absorption measurements were prepared by drop casting from the THF solution onto microscope slides. Steady-state fluorescence spectra from single crystals or polycrystalline samples were collected using a Spex Fluorolog Tau-3 fluorescence spectrophotometer. The solution samples were excited at 380 nm, and the spectra were collected from 390 to 700 nm at 296 K; the solid samples were excited at 410 nm, and the spectra were collected from 420 to 700 nm at 296 K.

6. Optical Microscopy. The samples were prepared by placing crystals onto microscope slides. To check the photoresponse of these crystals, images before irradiation were taken in transmission using a 40× 0.6 NA objective and visible light, after which they were irradiated by either 365 or 440 nm light for a few seconds and the images after irradiation were taken. The images were captured by a DCM300 digital camera.

RESULTS AND DISCUSSION

The synthesis of molecules **1**−**7** followed standard literature procedures for analogous anthracene derivatives, and the details are provided in the Supporting Information. After the molecules had been synthesized and purified, we had to grow crystals suitable for structure determination by X-ray diffraction (XRD). For some molecules (**1**, **5**), this could be accomplished using standard solution-based crystal growth techniques. For the other derivatives (**2**−**4**, **6**, **7**), however, solution growth yielded dendritic crystals or crystals with high concentrations of defects. For these molecules, we used a modified sublimation procedure to obtain crystals large enough for single crystal XRD measurements. In all cases, we succeeded in obtaining good quality single crystal structures consistent with our expectations of the 9AC motif. The single crystal XRD parameters and crystal structure data for all seven crystal structures determined in this work are summarized in Table 1.

We began our investigation of anthracene carboxylic acid derivatives by exploring the effect of COOH substitution at different points on the anthracene ring. We obtained crystals of anthracene derivatives with the carboxylic acid group located at the 1 and 2 positions, but neither of these crystals showed any reactivity when exposed to 365 nm radiation. The crystal structure of 1-anthracene carboxylic acid shows that the anthracene rings arrange themselves into an offset herringbone pair motif (Supporting Information, Figure S1).[21,22] The anthracenes form interleaved planar two-dimensional hydrogen bond networks, where the reactive anthracene rings are offset from each other. For a given pair of parallel anthracene rings, the central carbons are more than 6 Å apart, too far to permit the [4 + 4] photocyclization to occur. Using molecular mechanics simulations, we found that when the COOH group is placed at any point other than the 9-position on the anthracene ring, there is less steric interaction from the surrounding hydrogens and the COOH group can become almost coplanar with the anthracene

dx.doi.org/10.1021/cg200883b |*Cryst. Growth Des.* XXXX, XXX, 000–000

Table 1. Crystal Data and Structure Refinement for Triclinic 1−7

ID	anthracene-9-carboxylic acid (**1**)	10-fluoro-anthracene-9-carboxylic acid (**2**)	10-chloro-anthracene-9-carboxylic acid (**3**)	10-bromo-anthracene-9-carboxylic acid (**4**)
empirical formula	$C_{15}H_{10}O_2$	$C_{15}H_9Br_{0.05}F_{0.95}O_2$	$C_{15}H_9ClO_2$	$C_{15}H_9BrO_2$
formula weight	222.23	243.27	256.67	301.13
temperature (K)	296(2)	100(2)	100(2)	100(2)
wavelength (Å)	0.71073	0.71073	0.71073	0.71073
crystal system	triclinic	monoclinic	monoclinic	monoclinic
space group	$P\bar{1}$(#2)	$P2(1)/c$ (#14)	$P2(1)/$(#4)	$P2(1)/c$ (#14)
unit cell dimensions	a = 3.8896(19) Å, α = 101.784(7)°	a = 9.2885(14) Å, α = 90°	a = 3.8116(7) Å, α = 90°	a = 9.2037(6) Å, α = 90°
	b = 9.384(5) Å, β = 95.457(7)°	b = 3.7650(6) Å, β = 97.517(3)°	b = 31.453(6) Å, β = 90.463(3)°	b = 3.8638(3) Å, β = 96.7531(10)°
	c = 14.852(7) Å, γ = 90.220(7)°	c = 30.373(5) Å, γ = 90°	c = 9.2257(18) Å, γ = 90°	c = 31.580(2) Å, γ = 90°
volume (Å^3)	528.1(4)	1053.1(3)	1106.0(4)	1115.22(14)
Z	2	4	4	4
density (calculated) (Mg/m^3)	1.398	1.534	1.541	1.794
absorption coefficient (mm^{-1})	0.092	0.301	0.333	3.674
F(000)	232	501	528	600
crystal size	0.50 × 0.15 × 0.03 mm^3	0.55 × 0.08 × 0.02 mm^3	0.54 × 0.17 × 0.03 mm^3	0.51 × 0.20 × 0.03 mm^3
theta range for data collection	2.22−25.02°	2.21−29.13°	2.21−28.70°	2.23−29.57°
index ranges	$-4 \le h \le 4$, $-11 \le k \le 11$, $-16 \le l \le 17$	$-12 \le h \le 12$, $-5 \le k \le 5$, $-41 \le l \le 41$	$-5 \le h \le 5$, $-42 \le k \le 42$, $-12 \le l \le 12$	$-12 \le h \le 12$, $-5 \le k \le 5$, $-43 \le l \le 43$
reflections collected	4510	21009	22556	22753
independent reflections	1849 [R(int) = 0.0404]	2827 [R(int) = 0.0716]	5699 [R(int) = 0.0579]	3135 [R(int) = 0.0390]
completeness to theta = 29.13°	98.7%	99.9%	99.9%	99.9%
absorption correction	semiempirical from equivalents	semiempirical from equivalents	semiempirical from equivalents	semiempirical from equivalents
max and min transmission	0.9974 and 0.9557	0.9934 and 0.8518	0.9891 and 0.8416	0.9138 and 0.2579
refinement method	full-matrix least-squares on F^2	full-matrix least-squares on F^2	full-matrix least-squares on F^2	full-matrix least-squares on F^2
data/restraints/parameters	1849/0/157	2827/0/170	5699/1/331	3135/0/167
goodness-of-fit on F2	1.095	1.083	1.042	1.351
final R indices [$I > 2\sigma(I)$]	R_1 = 0.0882, wR_2 = 0.2265	R_1 = 0.0703, wR_2 = 0.1910	R_1 = 0.0503, wR_2 = 0.1268	R_1 = 0.0543, wR_2 = 0.1153
R indices (all data)	R_1 = 0.1109, wR_2 = 0.2399	R_1 = 0.0920, wR_2 = 0.2078	R_1 = 0.0561, wR_2 = 0.1313	R_1 = 0.0584, wR_2 = 0.1166
largest diff peak and hole	0.347 and −0.256 e·Å^{-3}	0.617 and −0.346 e·Å^{-3}	0.460 and −0.470 e·Å^{-3}	1.008 and −3.260 e·Å^{-3}

ID	10-methyl-anthracene-9-carboxylic acid (**5**)	10-phenyl-anthracene-9-carboxylic acid (**6**)	3-anthracen-9-yl-acrylic acid (**7**)
empirical formula	$C_{16}H_{12}O_2$	$C_{21}H_{14}O_2$	$C_{17}H_{12}O_2$
formula weight	236.26	298.32	248.27
temperature (K)	296(2)	100(2)	296(2)
wavelength (Å)	0.71073	0.71073	0.71073
crystal system	monoclinic	orthorhombic	monoclinic
space group	$P2(1)/c$ (#14)	$Pbca$ (#61)	$P2(1)/c$ (#14)
unit cell dimensions	a = 8.5743(3) Å, α= 90°	a = 7.1691(5) Å, α= 90°	a = 3.8919(4) Å, α= 90°
	b = 8.2539(3) Å, β= 94.9243(5)°	b = 13.5819(10) Å, β= 90°	b = 16.5883(15) Å, β= 93.7657(14)°
	c = 16.4805(6) Å, γ = 90°	c = 30.767(2) Å, γ = 90°	c = 19.0073(17) Å, γ = 90°
volume (Å^3)	1162.04(7)	2995.8(4)	1224.5(2)
Z	4	8	4
density (calculated) (Mg/m^3)	1.350	1.323	1.347
absorption coefficient (mm^{-1})	0.088	0.084	0.088
F(000)	496	1248	520
crystal size	0.44 × 0.42 × 0.18 mm^3	0.58 × 0.07 × 0.04 mm^3	0.54 × 0.07 × 0.05 mm^3
theta range for data collection	2.38−29.13°	2.65−25.67°	1.63−28.70°
index ranges	$-11 \le h \le 11$, $-11 \le k \le 11$, $-22 \le l \le 22$	$-8 \le h \le 8$, $-16 \le k \le 16$, $-37 \le l \le 36$	$-5 \le h \le 5$, $-22 \le k \le 22$, $-25 \le l \le 25$
reflections collected	16250	46262	16995

dx.doi.org/10.1021/cg200883b |Cryst. Growth Des. XXXX, XXX, 000–000

Table 1. Continued

ID	10-methyl-anthracene-9-carboxylic acid (**5**)	10-phenyl-anthracene-9-carboxylic acid (**6**)	3-anthracen-9-yl-acrylic acid (**7**)
independent reflections	3129 [R(int) = 0.0152]	2848 [R(int) = 0.0844]	3162 [R(int) = 0.0353]
completeness to theta = 29.13°	100.0%	100.0%	100.0%
absorption correction	semiempirical from equivalents	semiempirical from equivalents	semiempirical from equivalents
max and min transmission	0.9842 and 0.9623	0.9966 and 0.9527	0.9955 and 0.9542
refinement method	full-matrix least-squares on F^2	full-matrix least-squares on F^2	full-matrix least-squares on F^2
data/restraints/parameters	3129/0/167	2848/0/210	3162/0/175
goodness-of-fit on F2	1.057	1.106	1.003
final R indices [$I > 2\sigma(I)$]	$R_1 = 0.0467$, $wR_2 = 0.1405$	$R_1 = 0.0518$, $wR_2 = 0.1243$	$R_1 = 0.0418$, $wR_2 = 0.0988$
R indices (all data)	$R_1 = 0.0532$, $wR_2 = 0.1497$	$R_1 = 0.0731$, $wR_2 = 0.1383$	$R_1 = 0.0787$, $wR_2 = 0.1201$
largest diff peak and hole	0.317 and −0.228 e·Å^{-3}	0.268 and −0.268 e·Å^{-3}	0.221 and −0.231 e·Å^{-3}

ring. This permits the type of planar networks seen in the 1-anthracene carboxylic acid crystal. We were unable to grow crystals of 2-anthracene carboxylic acid suitable for X-ray structure determination. Given the empirical fact that only the 9-substituted member of this family appears to be photoreactive, we decided to investigate its derivatives in more detail.

In contrast to the molecules described above, interactions with hydrogens at the 1 and 8 positions force the COOH group to rotate ∼55° out of plane in 9AC (**1**). This rotation prevents formation of the planar two-dimensional crystal networks seen in 1-anthracene carboxylic acid. 9AC can crystallize in two polymorphs: monoclinic[23,24] and triclinic.[25] Using powder XRD, we found that many solution-grown crystals contain both forms in varying amounts. For example, our earlier powder XRD measurements of nanorods grown from THF contain peaks due to both monoclinic and triclinic forms.[14] After some trial-and-error, we found that pure triclinic crystals could be grown using xylenes, while pure monoclinic crystals could be grown from ethyl acetate. The detailed structure of the monoclinic polymorph can be found in the Cambridge Database and is illustrated in Figure 1a,b. The crystal structure of the triclinic form is presented in this paper for the first time and is shown in Figure 1c,d. In both crystals, the 9AC molecules stack on top of each other, as shown in Figure 1b,d. The rotated COOH groups can participate in hydrogen bonding with molecules in neighboring stacks, resulting in hydrogen bonded stack pairs rather than the offset herringbone pairs formed by anthracenes with coplanar COOH groups. It is these stacked 9AC molecules that provide the correct orientation and distance for the [4 + 4] photodimerization to take place. Despite the similarities, there are two significant differences between the two polymorphs, which are highlighted in Figure 1. In the monoclinic form, neighboring pair stacks are rotated by 62.7° when viewed from the top (Figure 1a), and these stacks also form a 23.2° angle when the stack axes are compared (Figure 1b). In contrast, neighboring pair stacks in the triclinic form are completely parallel to each other, both when viewed from the top and when viewed from the side, as shown in Figure 1c,d. It is doubtful that these differences in packing change the photochemistry of individual anthracene pairs, since the distances between adjacent anthracenes, which participate in the [4 + 4] photodimerization, are the same in both crystal polymorphs at 3.9 Å. The presence of two different polymorphs may help explain the variability seen in the photoresponses of nanorods of **1** grown in THF,[15] where both polymorphs are possible.

Since placing the COOH group at the 9-position is vital for making a reactive crystal, we reasoned that modifying the reactivity of the crystal would require substitution at other positions around the anthracene ring. Changing the chemical group at the 10-position exactly opposite the COOH is a synthetically tractable approach that provides an opportunity to modify the steric properties of the molecule without dramatically changing its electronic properties. One of our hopes was that by placing a bulkier group at the 10-position, we could further destabilize the photodimer and decrease its dissociation time. When the hydrogen at the 10-position is replaced with a halogen atom (F, Cl, Br), the distance between the anthracenes changes by less than 3.5% relative to **1**. The major change in the crystal packing involves the relative tilt angles of neighboring stacks, as shown in Figures 2 and 3. Whereas in triclinic **1** the H-bonded pair stacks line up parallel to each other, in **2**−**4** the packing is more similar to monoclinic **1**, with the pair stacks tilted vertically with respect to each other (Figure 2a−c). This is true whether or not the top view shows the anthracene stacks rotated from each other. It is only when we put larger substituents at the 10-position (methyl = **5** or phenyl = **6**) that we see a disruption of the 9AC stacking motif. In **5**, the methyl group substituents lead to a reversal of the head-to-head stacking and instead we find the more common head-to-tail pairwise arrangement, as shown in Figure 3a. The parallel anthracene rings are offset from each other and spaced farther apart (4.84 Å versus 3.90 Å in 9AC between two 9-position carbons in the pair). This arrangement of neighboring anthracenes is not conducive for the [4 + 4] photodimerization reaction, which is generally limited to pairs with a center-to-center distance of 4.7 Å or less.[26] In **6**, the anthracenes adopt the head-to-head pairwise arrangement shown in Figure 3b. But now the hydrogen-bonding arrangement is completely different, with a single COOH group interacting with two different molecules as illustrated by the green dotted line in Figure 3b, spreading the anthracene rings too far apart to photodimerize. In crystals of **5** and **6**, shifting of the molecules to spatial positions more amenable for reaction is presumably prevented by the hydrogen bonds that lock the anthracenes in place. In addition to modifying the 10-position, we also made one molecule with a vinylene group separating the COOH from the main anthracene ring (molecule **7**) in order to examine whether this separation could modify the standard H-bonding network seen in all the 9AC derivatives. This molecule exhibits the familiar stacking motif seen in compounds **1**−**4** as seen in Figure 3c. It should be emphasized that, in analogy with **1**, it is possible that other polymorphs of **2**−**7** exist. We were unable to detect them,

dx.doi.org/10.1021/cg200883b |*Cryst. Growth Des.* XXXX, XXX, 000–000

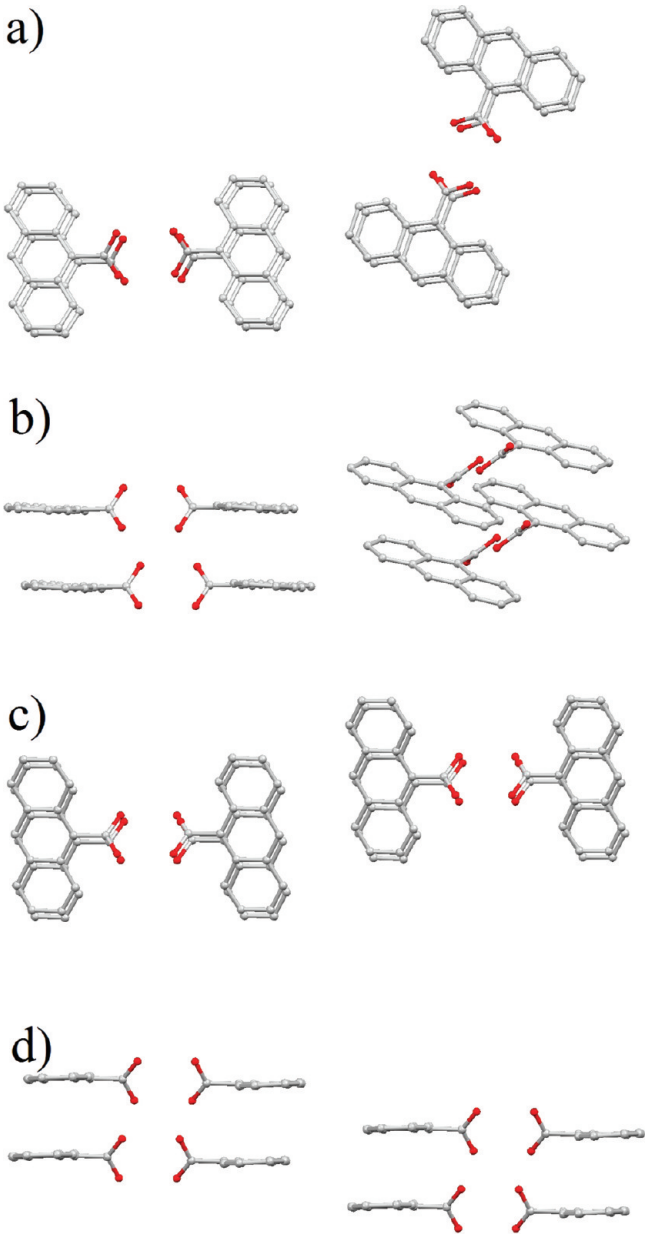

Figure 1. Crystal structures and packing of (a) top view of monoclinic **1** (anthracene-9-carboxylic acid); (b) side view of monoclinic **1**; (c) top view of triclinic **1**; (d) side view of triclinic **1**.

however, and the structures in Figure 2 are consistent with the photophysics described below.

Clearly, different substituents on 9AC can affect the crystal packing. The next question is how the photophysical properties, including photoreactivity, are affected. The photophysics in the solid-state will be affected by both intermolecular interactions and by intramolecular relaxation. Figure 4 shows the steady-state absorption and fluorescence spectra for compounds **1**−**7** in THF solution. The spectra for compounds **1**−**6** are all quite similar, with the characteristic anthracene vibronic progression in the absorption spectrum and the broadened, shifted fluorescence that arises from charge-transfer interactions with the carbonyl group in the excited state.[27] The only significant difference between the spectra is the red-shift of both the absorption and fluorescence spectra as more electron-rich substituents

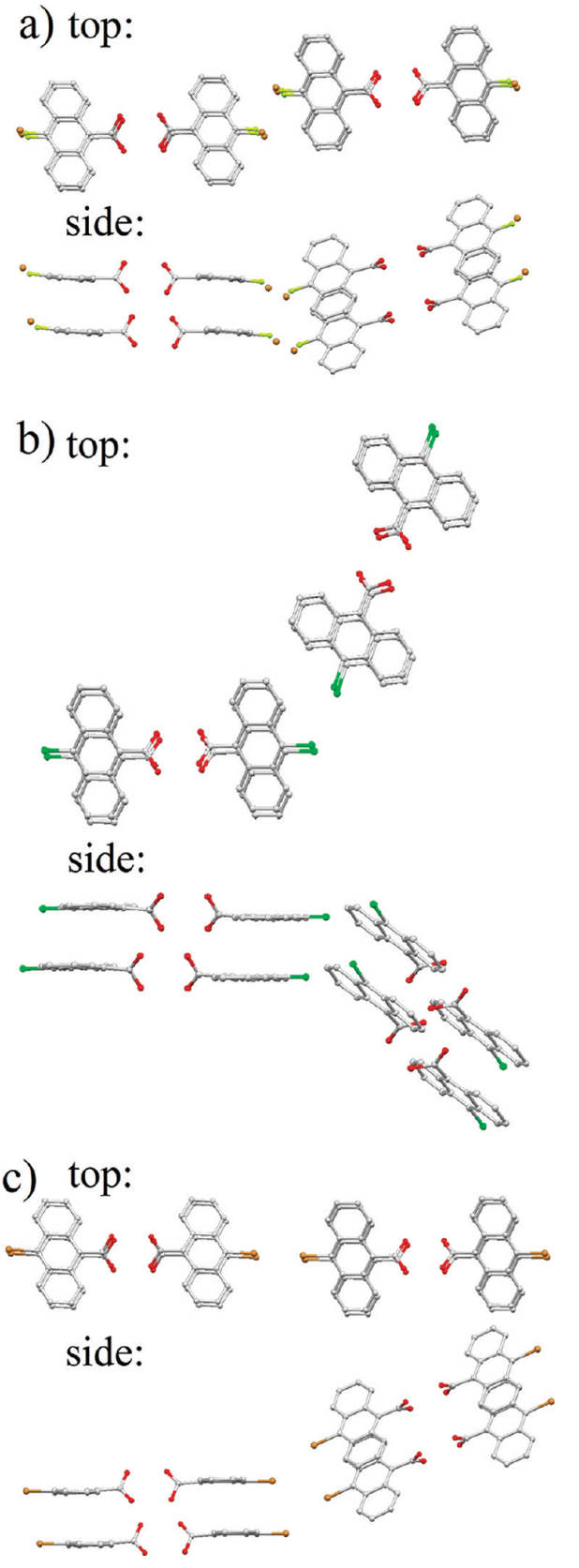

Figure 2. Top and side views of crystal structures of anthracene carboxylic acid derivatives: (a) 10-fluoro-anthracene-9-carboxylic acid **2** (with 5% disorder of 10-bromo-anthracene-9-carboxylic acid **4**); (b) 10-chloro-anthracene-9-carboxylic acid **3**; (c) 10-bromo-anthracene-9-carboxylic acid **4**.

dx.doi.org/10.1021/cg200883b |*Cryst. Growth Des.* XXXX, XXX, 000–000

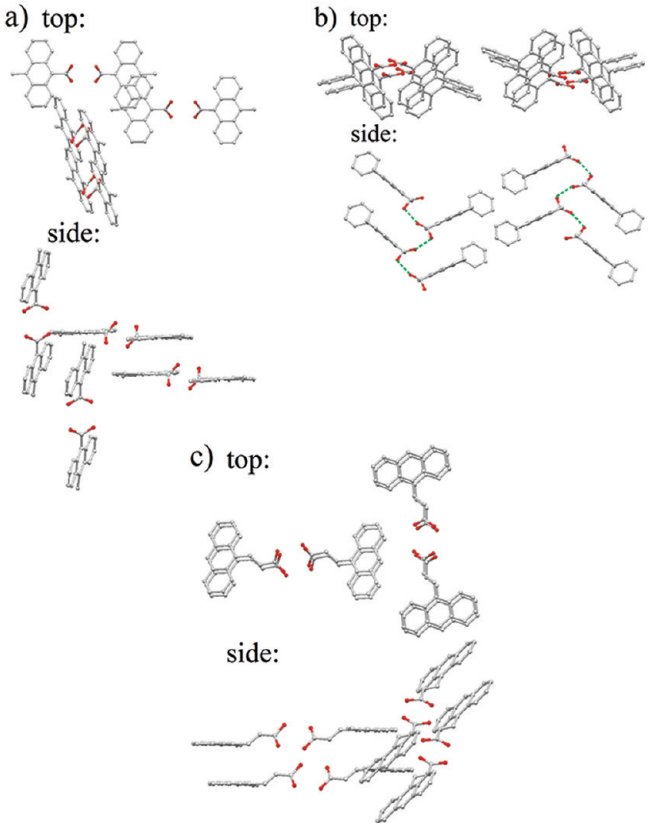

Figure 3. (a) 10-Methyl-anthracene-9-carboxylic acid **5**; (b) 10-phenyl-anthracene-9-carboxylic acid **6** (the green dotted line in the side view signify hydrogen bond chain); (c) 3-anthracen-9-yl-acrylic acid **7**.

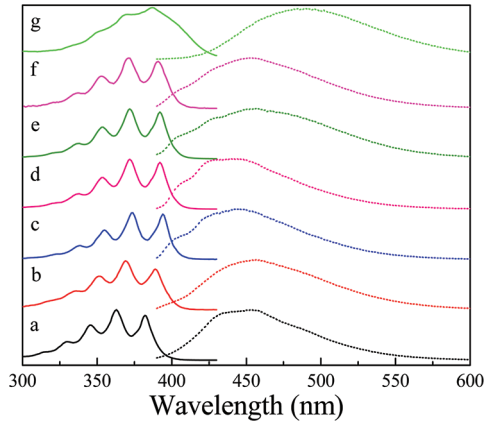

Figure 4. Absorption and emission spectroscopy of 9-anthracene carboxylic acid (9AC) and its derivatives in THF solutions: (a) anthracene-9-carboxylic acid **1**; (b) 10-fluoro-anthracene-9-carboxylic acid **2**; (c) 10-chloro-anthracene-9-carboxylic acid **3**; (d) 10-bromo-anthracene-9-carboxylic acid **4**; (e) 10-methyl-anthracene-9-carboxylic acid **5**; (f) 10-phenyl-anthracene-9-carboxylic acid **6**; (g) 3-anthracen-9-yl-acrylic acid **7**. The solid line plots are the absorption spectra, and the dotted line plots are the fluorescence spectra.

are placed at the 10-position. For **7**, this conjugation effect is very pronounced, and there is additional broadening in the absorption spectrum and a much larger Stokes shift, by almost 50 nm, than in the other compounds. When these molecules are

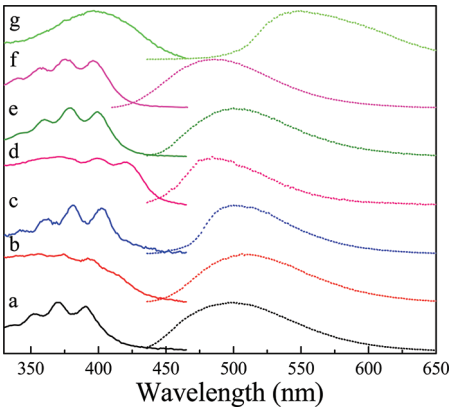

Figure 5. Absorption and emission spectroscopy of 9-anthracene carboxylic acid (9AC) and its derivatives in the solid state: (a) anthracene-9-carboxylic acid **1**; (b) 10-fluoro-anthracene-9-carboxylic acid **2**; (c) 10-chloro-anthracene-9-carboxylic acid **3**; (d) 10-bromo-anthracene-9-carboxylic acid **4**; (e) 10-methyl-anthracene-9-carboxylic acid **5**; (f) 10-phenyl-anthracene-9-carboxylic acid **6**; (g) 3-anthracen-9-yl-acrylic acid **7**. The solid line plots are the absorption spectra, and the dotted line plots are the fluorescence spectra.

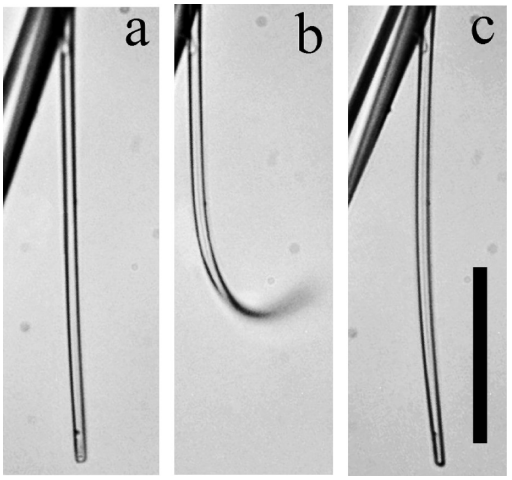

Figure 6. Optical microscopy images of a microneedle crystal composed of 10-fluoro-anthracene-9-carboxylic acid **2**: (a) before irradiation; (b) after a few seconds of 440 nm irradiation; (c) recovery after 30 min. The scale bar is 50 μm.

examined as polycrystalline films on a glass surface, there is considerably more variation in their spectral properties, as shown in Figure 5. In all cases, the absorption spectrum shifts by only 10−20 nm, as expected from the solid-state solvatochromic effect.[28] The fluorescence undergoes a much larger shift of 50 nm or more. This large Stokes shift of the fluorescence is indicative of excimer formation, as is often seen in π-stacked anthracene crystals. The loss of structure in the absorption spectra of **2** and **4** is most likely due to scattering effects in the films. The steady-state spectra in both dilute liquid solution and in the solid films suggest that the overall electronic structures are similar for molecules **1**−**6**, and that gross changes in electronic structure (resulting from formation of H- or J-aggregates, for example) do not occur when the molecules crystallize. The presence of excimer emission is expected in these π-stacked systems and is probably an indication of the

dx.doi.org/10.1021/cg200883b |*Cryst. Growth Des.* XXXX, XXX, 000–000

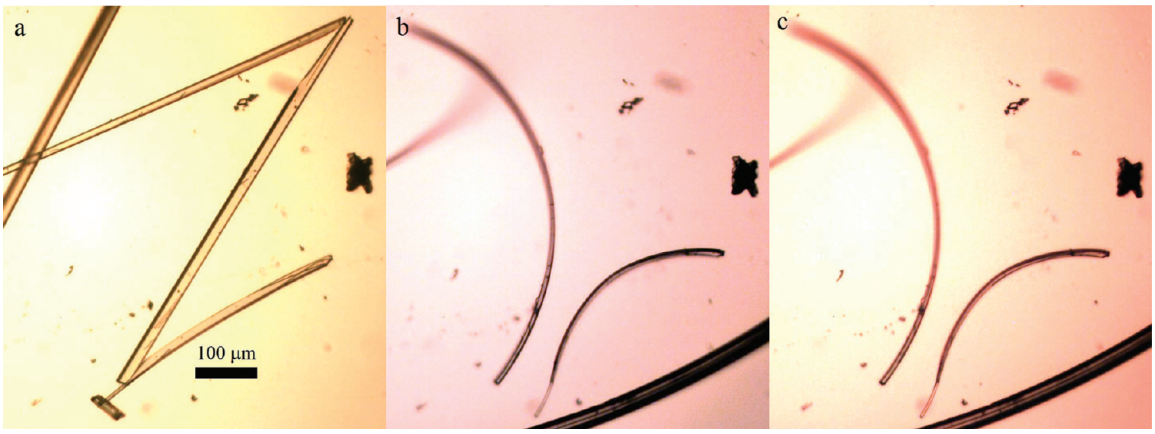

Figure 7. Optical microscopy images of bulk crystals of **7**: (a) before irradiation; (b) after 1 h irradiation. The thickest crystal originally on the top left corner of (a) jumped to the bottom right corner of (b) and bent. The other three crystals bent in place. (c) The bent crystals from panel (b) after 16 h; there is no sign of recovery. The scale bar in (a) is 100 μm.

electronic interactions in the excited state that facilitate the [4 + 4] dimerization reaction.[29−31]

Despite the presence of excimer emission in all crystals, only **1**, **2**, and **7** were found to be photoreactive. For the other molecules (**3**−**6**), no change in emission or physical shape was observed under even prolonged (>1 h) irradiation. Since the focus of this paper is potential photomechanical materials, we now discuss and compare the properties of the photoreactive crystals in detail. In both its triclinic and monoclinic forms, compound **1** reacts rapidly when exposed to light in the range 365−440 nm from a microscope mercury lamp. This photoreaction results in the loss of its bright green-yellow fluorescence and the appearance of a much less intense, blue fluorescence which we have attributed to unreacted monomers.[13,32] This change in emission is accompanied by the fracture and jumping of individual crystals when viewed under a microscope. After several minutes, the green-yellow fluorescence recovers and the process can be repeated. Crystallites composed of **2** showed similar photobleaching behavior as **1**, and this was usually accompanied by a deformation of the crystal. The deformation was reversible in **2**, as shown in Figure 6 for a microneedle grown by sublimation. Crystals of **7** could also deform under irradiation, as shown in Figure 7, but this reaction was not reversible at room temperature on any time scale, making this molecule of less interest as a potential photoactuator. Both **2** and **7** showed a much slower response to 365 nm radiation than **1**. The bending of the crystal of **2** shown in Figure 6 only occurred after several minutes of irradiation. The response of crystals composed of **7** occurred on even longer time scales, requiring 40−80 min of light exposure to generate the shape changes seen in Figure 7. If we assume that the absorption cross sections at 365 nm are approximately equal and that the deformation rate is proportional to the amount of photodimer generated in the crystal,[15] then these changes in rate should be directly proportional to the reaction yield. This yield has been measured to be 7 ± 1% in monoclinic **1**,[24] so the photochemical reaction yields are likely to be 1% or less in **2**. For **7**, the reaction yield may be higher since the absorption is red-shifted, and our assumption that the cross section is equal to that of **1** at 365 nm is less likely to be valid. The lower reaction yield is accompanied by much slower recovery time in **2**, where the recovery time (20−30 min) is roughly an order of magnitude longer than what has been observed in **1**.

One qualitative observation is that crystals of **2** appear to be more plastic than crystals of **1** and less prone to shatter under irradiation. Our hope was that this greater elasticity would lead to improved fatigue resistance so that an actuator based on this material could be used repeatedly. A sequence of bending-relaxation images for a microneedle composed of **2** is given in the Supporting Information and shows that this needle could undergo three bending sequences before it became unresponsive. This loss of responsivity is comparable to what we observed previously for 9AC nanorods in air and ascribed to the photochemical reaction with oxygen to form an endoperoxide.[13] We have observed better fatigue resistance for crystals of **1** when they are submerged in aqueous solutions where the O_2 concentration is lower, and it is likely that the fatigue resistance of **2** could also be improved by the rigorous exclusion of O_2 and other species that lead to photochemical side reactions. At the present time, however, it does not appear that these materials, based on the anthracene [4 + 4] photodimerization, will prove to be as robust as structures based on photochromic diarylethene derivatives.[33]

The exact molecular-level mechanism for the crystal deformation remains unclear. Ideally, a knowledge of the before (monomer) and after (dimer) crystal structures, along with the orientation of the crystal within the microstructure, should provide insight into the mechanism of its photodeformation. In practice, we have found that analysis of the photomechanical response of this class of crystals is complicated by the presence of metastable intermediate states.[11] We did not attempt to correlate the direction of bending in **2** with crystal orientation. It appeared to be random with respect to direction, implying that crystal orientation did not absolutely fix the bend direction. For **1** and **2**, the dimer crystal reverts back to the monomer on a time scale shorter than that required to obtain a single crystal XRD structure. Performing a low temperature photoconversion followed by an XRD experiment is possible but beyond the scope of this paper. Compound **7** is the only molecule where the photodimer product is sufficiently stable to permit an attempt to measure the single crystal XRD structure of the dimer product crystal. We analyzed several different crystals of photoreacted **7** and found that in every case the crystal structure obtained was indistinguishable from the monomer crystal shown in Figure 3c. There were indications of possible

dx.doi.org/10.1021/cg200883b |*Cryst. Growth Des.* XXXX, XXX, 000–000

Table 2. Fluorescence Lifetimes of Solid Anthracene Carboxylic Acid Derivatives

9AC derivatives	lifetime (ns)		crystal photoreactivity	reversibility	anthracene separation (Å)[a]	stack angle (°)[b]
1 monoclinic	35 ± 4		yes	yes	3.90	23.2
1 triclinic	35 ± 4		yes	yes	3.89	0
2	9.3 ± 0.9		yes	yes	3.77	48.3
3	15 ± 2		no		3.81	44.6
4	2.5 ± 0.3		no		3.86	52.5
5	t_1 = 1.6 ± 0.2	A_1 = 0.49	no		4.84	75.6
	t_2 = 8.0 ± 0.8	A_2 = 0.51				
6	t_1 = 1.3 ± 0.1	A_1 = 0.47	no		7.17	67.6
	t_2 = 3.1 ± 0.3	A_2 = 0.53				
7	not measured		yes	no	3.89	52.5

[a] The separation distance was measured between the two 9-position carbons for two paired anthracene carboxylic acid molecules within a single stack. [b] The stack angle was the angle between two anthracene planes within two different stacks which are not hydrogen bonded to each other, and which tilt in different directions.

dimerization from the calculated difference electron density map, which showed 3−4 weak electron density peaks between the two middle rings of **7** from several photoreacted crystals. But even when a two-component analysis was attempted, similar to what we successfully used to determine an intermediate structure in the solid-state reaction of 9-tertbutylanthracene ester,[11] we could not resolve any molecular structure that resembled the expected photodimer. This is not totally surprising in light of the fact that the photodimerization yield in these one-dimensional stacked crystals cannot approach 100% due to statistical considerations. The theoretical maximum is 87%,[34,35] but in monoclinic **1** the actual yield is closer to 75%.[24] This means that even in the best case, there will be a significant amount of monomer crystal left over after the photoreaction. In the case of **7**, it appears that this left-over monomer dominates the XRD data and prevents the determination of the dimer crystal structure. The lack of structural information on the dimer product crystal prevents us from positing a molecular-level pathway for how photodimerization within the molecular stacks leads to larger scale crystal deformation.

If we now consider the group of unreactive molecules, the lack of photoreactivity in **5** and **6** can be easily rationalized on the basis of the large distances between the anthracene rings, the reason that **3** and **4** do not photodimerize is less clear. We were concerned that the presence of the heavy atoms Cl and Br might lead to competing nonradiative decay processes, like intersystem crossing, so we measured the excited state lifetimes of all the solids at room temperature using fluorescence decays. We concentrated on the solid-state fluorescence lifetimes, since it is clear from Figures 3 and 4 that the emissive excimer in the solids is a new electronic state, distinct from the monomer singlet state that determines the emission properties in solution. The results of these measurements are given in Table 2, along with other relevant parameters for this family of compounds. All the molecules studied had lifetimes in the nanosecond range, indicating that dimerization does not occur on ultrafast (sub-nanosecond) time scales. The lifetime of **1** was 35 ± 4 ns for both the triclinic and monoclinic polymorphs to within the experimental error. The measured dimerization quantum yield of monoclinic **1** in the solid state of 7 ± 1%[24] suggests that the rate of dimerization is on the order of several hundred nanoseconds. This relatively slow reaction rate suggests that the [4 + 4] dimer formation is a minor channel for excited state relaxation, competing with many other channels. If the photochemical reaction rate is similar for **1**−**4**, as seems likely given their similar crystal structures, then fewer competing channels should lead to both a longer fluorescence lifetime and a larger photoreaction yield. In this limit, a longer fluorescence lifetime should result in more efficient photoproduct formation. But the lifetime of the unreactive **3** (15 ± 2 ns) is longer than that of the reactive **2** (9.3 ± 1 ns), while that of **4** (2.5 ± 0.3 ns) is shorter, so there is no clear trend in excited state lifetime with halogen substitution. Molecules **5** and **6** had biexponential fluorescence decays that were the most rapid of all the 10-substituted compounds, despite their lack of heavy atoms or photoreactivity. It appears that fast intersystem crossing or internal conversion in the Cl- and Br-substituted anthracenes does not provide a straightforward explanation for their lack of photoreactivity.

Since the fluorescence lifetime measurements do not provide a clear explanation for the reactivity trends in the halogen-substituted 9AC series, we now consider steric effects. Compounds **1**−**4** provide a rare example of a situation where halogen substitution does not change the overall crystal packing, which is locked in place by the hydrogen-bond interactions. The reactive compounds' H and F atoms have atomic radii of 25 and 75 pm, respectively, while the Cl and Br atoms have radii of 100 and 114 pm, respectively. The Cl and Br substituents may simply be too large to permit the dimers to form due to steric repulsion. Attempts to calculate the energy differences of the monomer pair versus the covalent dimer were unsuccessful due to their ill-defined geometries in the crystal environment, but steric effects are known to be important in solution phase photodimerization reactions of anthracene derivatives.[31,36] But if larger atoms at the 10-position destabilize the dimer, we still are at a loss to explain why **2** has a much longer dissociation and recovery time than **1**. We expected the F−F repulsion to destabilize the dimer and result in a faster "reset" time but observed the opposite effect. One possible explanation is that the highly electronegative F atom interacts with other atoms of π-electron clouds within the crystal in new ways after photodimerization that act to stabilize the overall dimer structure. A detailed study of the crystal interactions before and after dimerization is beyond the scope of this paper. For now, we simply emphasize that steric considerations, like the fluorescence lifetime data described in the preceding paragraph, can explain some but not all of the trends observed experimentally.

dx.doi.org/10.1021/cg200883b |*Cryst. Growth Des.* XXXX, XXX, 000–000

CONCLUSION

The goal of this work is to explore how chemical modification of the 9AC basic unit affects crystal packing and photoreactivity. One goal was to find materials with improved photomechanical properties, for example, faster recovery times. We found that substitution at the 10-position often led to a complete loss of photoreactivity due to changes in either the crystal packing (**5** and **6**) or steric repulsion (**3** and **4**). Of the remaining candidates, crystals of **7** showed good photoreactivity and a lack of fracture but no recovery after irradiation. Compound **2**, where the H has been replaced by an F atom, was the closest to 9AC in terms of its photomechanical behavior, but with a much longer recovery time. Attempts to self-consistently rationalize observed trends in terms of excited state lifetimes or steric effects were only partially successful. The present paper illustrates how competing effects complicate the search for an improved photomechanical material based on the 9AC framework. Although our search did result in the discovery of a new reversible photomechanical crystal (**2**), its properties are not obviously superior to that of **1**. While organic chemistry provides unlimited opportunities for chemical modification of the active chromophore, balancing various factors such as electronic relaxation, steric interactions, and crystal packing remain a challenge for engineering materials based on molecular crystals. One possible strategy to overcome these competing effects is to use cocrystals to engineer better control over assembly in the solid state.[37,38]

ASSOCIATED CONTENT

Supporting Information. Synthesis of 9-anthracene carboxylic acid derivatives **2**−**7**; crystal structure of 1-anthracene carboxylic acid; crystallographic information files. This material is available free of charge via the Internet at http://pubs.acs.org.

AUTHOR INFORMATION

Corresponding Author

*E-mail: christopher.bardeen@ucr.edu.

ACKNOWLEDGMENT

This research was supported by the National Science Foundation, Grant DMR-0907310. Fluorescence lifetime measurements were performed on an instrument purchased with support from the National Science Foundation, Grant CRIF-0840055. The electron microscopy measurements were done at the Center for Advanced Materials and Microscopy (CFAMM) at UC Riverside. R.O.A.-K. acknowledges the support of KSAU-HS/KAIMRC through Grants RC08/093 and RC10/104 and King Abdulaziz City for Science and Technology (KACST) through Grant AT-435-30.

REFERENCES

(1) Finkelmann, H.; Nishikawa, E.; Pereira, G. G.; Warner, M. *Phys. Rev. Lett.* **2001**, *87*, 015501/1.
(2) Ikeda, T.; Mamiya, J.; Yu, Y. *Ang. Chem. Int. Ed.* **2007**, *46*, 506.
(3) Oosten, C. L. v.; Bastiaansen, C. W. M.; Broer, D. J. *Nat. Mater.* **2009**, *8*, 677.
(4) Lange, C. W.; Foldeaki, M.; Nevodchikov, V. I.; Cherkasov, V. K.; Abakumov, G. A.; Pierpont, C. G. *J. Am. Chem. Soc.* **1992**, *114*, 4220.
(5) Irie, M.; Kobatake, S.; Horichi, M. *Science* **2001**, *291*, 1769.
(6) Kobatake, S.; Takami, S.; Muto, H.; Ishikawa, T.; Irie, M. *Nature* **2007**, *446*, 778.
(7) Koshima, H.; Ojima, N.; Uchimoto, H. *J. Am. Chem. Soc.* **2009**, *131*, 6890.
(8) Naumov, P.; Kowalik, J.; Solntsev, K. M.; Baldridge, A.; Moon, J.-S.; Kranz, C.; Tolbert, L. M. *J. Am. Chem. Soc.* **2010**, *132*, 5845.
(9) Uchida, K.; Sukata, S.; Matsuzawa, Y.; Akazawa, M.; Jong, J. J. D. d.; Katsonis, N.; Kojima, Y.; Nakamura, S.; Areephong, J.; Meetsma, A.; Feringa, B. L. *Chem. Commun.* **2008**, 326.
(10) Al-Kaysi, R. O.; Muller, A. M.; Bardeen, C. J. *J. Am. Chem. Soc.* **2006**, *128*, 15938.
(11) Zhu, L.; Agarwal, A.; Lai, J.; Al-Kaysi, R. O.; Tham, F. S.; Ghaddar, T.; Mueller, L.; Bardeen, C. J. *J. Mater. Chem.* **2011**, *21*, 6258.
(12) Ito, Y.; Fujita, H. *J. Org. Chem.* **1996**, *61*, 5677.
(13) Al-Kaysi, R. O.; Bardeen, C. J. *Adv. Mater.* **2007**, *19*, 1276.
(14) Al-Kaysi, R. O.; Dillon, R. J.; Zhu, L.; Bardeen, C. J. *J. Colloid. Interfac. Sci.* **2008**, *327*, 102.
(15) Good, J. T.; Burdett, J. J.; Bardeen, C. J. *Small* **2009**, *5*, 2902.
(16) Zhu, L.; Al-Kaysi, R. O.; Bardeen, C. J. *J. Am. Chem. Soc.* **2011**, *133*, 12569.
(17) 2008/1 ed.; Bruker AXS Inc.: Madison, WI, 2008.
(18) 2008/4 ed.; Bruker AXS Inc.: Madison, WI, 2008.
(19) 2009.5−1 ed.; Bruker AXS Inc.: Madison, WI, 2009.
(20) V7.60A ed.; Bruker AXS Inc.: Madison, WI, 2009.
(21) Fitzgerald, L. J.; Gerkin, R. E. *Acta Crystallogr. Sect. C* **1997**, *53*, 1080.
(22) Fitzgerald, L. J.; Gerkin, R. E. *Acta Crystallogr. Sect. C* **1996**, *52*, 1838.
(23) Fitzgerald, L. J.; Gerkin, R. E. *Acta Crystallogr. Sect. C* **1997**, *53*, 71.
(24) More, R.; Busse, G.; Hallmann, J.; Paulmann, C.; Scholz, M.; Techert, S. *J. Phys. Chem. C* **2010**, *114*, 4142.
(25) Heller, E.; Schmidt, G. M. J. *Isr. J. Chem.* **1971**, *9*, 449.
(26) Ramamurthy, V.; Venkatesan, K. *Chem. Rev.* **1987**, *87*, 433.
(27) Dey, J.; H., III, J. L.; Warner, I. M.; Chandra, A. K. *J. Phys. Chem. A* **1997**, *101*, 2271.
(28) Baldo, M. A.; Soos, Z. G.; Forrest, S. R. *Chem. Phys. Lett.* **2001**, *347*, 297.
(29) Stevens, B. *Adv. Photochem.* **1971**, *8*, 161.
(30) Charlton, J. L.; Dabestani, R.; Saltiel, J. *J. Am. Chem. Soc.* **1983**, *105*, 3473.
(31) Bouas-Laurent, H.; Castellan, A.; Desvergne, J.-P.; Lapouyade, R. *Chem. Soc. Rev.* **2001**, *30*, 248.
(32) MacFarlane, R. M.; Philpott, M. R. *Chem. Phys. Lett.* **1976**, *41*, 33.
(33) Morimoto, M.; Irie, M. *J. Am. Chem. Soc.* **2010**, *132*, 14172.
(34) Cohen, E. R.; Reiss, H. *J. Chem. Phys.* **1963**, *38*, 680.
(35) Even, J.; Bertault, M. *J. Chem. Phys.* **1999**, *110*, 1087.
(36) Castellan, A. *Compt. Rend. Ser. C* **1975**, *281*, 221.
(37) MacGillivray, L. R.; Papaefstathiou, G. S.; Friscic, T.; Hamilton, T. D.; Bucar, D. K.; Chu, Q.; Varshney, D. B.; Georgiev, I. G. *Acc. Chem. Res.* **2008**, *41*, 280.
(38) Kapadia, P. P.; Ditzler, L. R.; Baltrusaitis, J.; Swenson, D. C.; Tivanski, A. V.; Pigge, C. F. *J. Am. Chem. Soc.* **2011**, *133*, 8490.